Numerical and Parametric Analysis of Excess Pore Pressure Behaviors in Unreinforced Embankments on Soft Soils

Laura Zappellini Sassi
Civil engineering undergraduate student, UFSC, Florianópolis, Brazil, lazasassi@gmail.com

Naloan Coutinho Sampa
Professor, UFSC, Florianópolis, Brazil, naloan.sampa@ufsc.br

ABSTRACT: This study, the third in a series of three, examines the behavior of excess pore pressure in four unreinforced embankments on soft soils. To this end, numerical modeling using Abaqus software is employed. The embankments, comprising granular materials, have dimensions of 3.5 meters in height and 17 meters in width. The underlying soft soil layer extends horizontally for 30 meters, with thicknesses varying from 5 to 20 meters. The investigation assesses the influence of overconsolidation ratio, recompression index, and critical state slope on excess water pressure behaviors through four different normalization methods. The results indicate that variations in recompression index exert a more significant impact on excess pore pressure behaviors compared to those of overconsolidation ratio and critical state slope. The implications of these findings on slope performance and stability are discussed. Additionally, the study underscores the efficacy of Abaqus software in modeling geotechnical problems.

KEYWORDS: Abaqus, Excess Pore Pressure, Effective Stress, Numerical Analysis, Parametric Analysis, Soft Soil, Unreinforced Embankments.

1 INTRODUCTION

Numerous investigations have explored the impact of pore pressure on the stability and compressibility of embankments on soft soils (De Freitas, 2019; Baroni, 2016; Dominoni, 2011, and others). One-dimensional consolidation theory, pioneered by Terzaghi (1914, 1925) and further developed by Terzaghi and Fröhlich (1936), postulates linear stress-strain relationships to elucidate consolidation phenomena. This theory correlates variations in pore pressure, effective vertical stress, and void ratio (Budhu, 2010).

The construction of embankments over soft soils requires continuous monitoring of excess pore pressure, especially during the loading phase. According to the principle of effective stress, raising the embankment generates excess pore pressure in the soft soil, thus changing the magnitude of the effective stress. The excess pore pressure can be positive or negative, depending on the degree of overconsolidation of the soil. Therefore, the assessment of excess pore pressure and effective stress during and after embankment construction can guide the rate of embankment elevation and provide a more accurate analysis of the change in strength and factor of safety over time (Coutinho, 1986; Ortigão, 1980; De Freitas, 2019).

Depending on the rate of embankment elevation and the properties of the soft soil, consolidation may begin during the embankment construction phase as excess pore pressure is dissipated, increasing strength. As a result, stability analyses of embankments on soft soils performed in terms of effective stresses require both the effective soil strength parameters (c' and ϕ') and pore pressure values. Pore pressures generated during and after construction are more difficult to estimate accurately in field, even when piezometers are used in instrumented embankments.

In recent decades, the use of numerical modeling for the analysis of geotechnical engineering problem has increased significantly. This includes the analysis of settlements in embankments on soft soils, with an emphasis on the dissipation of excess pore pressure and the increase in effective stress. This paper evaluates the influence of variation in overconsolidation ratio (OCR), recompression index (κ), and critical state slope (M) on pore pressure and effective stress during and after the construction of four unreinforced embankments.

XXI Congresso Brasileiro de Mecânica dos Solos e Engenharia Geotécnica
X Simpósio Brasileiro de Mecânica das Rochas
X Simpósio Brasileiro de Engenheiros Geotécnicos Jovens
24 a 27 de setembro de 2024 – Balneário Camboriú/SC

2   Models Description

The numerical analysis of four unreinforced embankments on soft soils was performed using Abaqus software and assuming the plane strain condition. The 2D models consisted of a 3.5 m deep and 17 m long embankment of granular material with a slope of 1:2 (vertical to horizontal) over a soft clay layer 30 m long and 5 to 20 m thick. Due to the symmetry of the model, only half of the domain was simulated, as shown in Figure 1, where H_s represents the thickness of the soft soil layer.
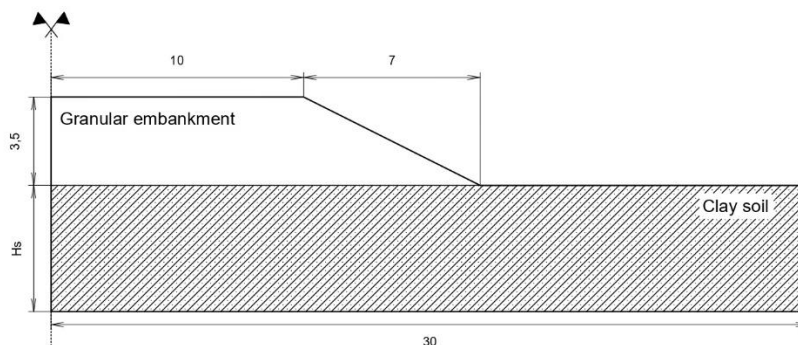

Figure 1. Half-domain of the numerical model of the embankment on the soft soil, in m.

2.2   Geotechnical Parameters

The soft clay was modeled as a homogeneous solid with elastoplastic behavior using the Modified Cam Clay plasticity criterion. Conversely, the granular embankment material was simulated in a dry state as a homogeneous solid body using the Mohr-Coulomb criterion. The geotechnical parameters for both the granular material and the clay soil are given in Table 1, where the clay parameters are typical of certain regions in Florianópolis, Brazil, as presented by Oliveira, 2006 and Baran, 2014.

Table 1. Geotechnical parameters of the soft soil and granular material.

Granular material of the embankment		Clay soil	
Parameter	Value	Parameter	Value
Initial void ratio - e_0	0.65	Initial void ratio - e_0	2.5
Bulk unit weight - γ (kN/m³)	20	Bulk unit weight - γ (kN/m³)	15
Cohesion - c (kN/m²)	2	Recompression index - κ	0.065
Internal friccional angle - ϕ (°)	30	Poisson's ratio - ν	0.33
Dilatancy angle - ψ (°)	0	Compression index - λ	0.65
Elastic Module - E (kN/m²)	1000	Slope of the critical state line - M	1
Poisson's ratio - ν	0.3	Overconsolidation ratio - OCR	0.75, 1.0, 1.5, 3.0
Permeability coefficient - k (m/s)	0.01	Size of the yield surface in the wet side - β	1
		Ratio of the flow stress - K	1
		Permeability coefficient - k (m/s)	2.50E-08
		Lateral earth pressure at rest – $K_0 = 1 - \operatorname{sen} \phi$	0.57

2.3   Simulation Sequences

The numerical simulations consisted of three stages, reflecting the sequential construction process of the single-phase embankments. The first stage involved the application of the Body Force option to stablish the initial geostatic stresses within the soft soil. The second stage then involved the gradual construction of the embankment to a height of 3.5 meters over a period of one month. Finally, the third phase involved monitoring the embankment's performance, including measuring vertical and horizontal displacements and excess pore water pressure, over a period of 48 months (4 years).

XXI Congresso Brasileiro de Mecânica dos Solos e Engenharia Geotécnica
X Simpósio Brasileiro de Mecânica das Rochas
X Simpósio Brasileiro de Engenheiros Geotécnicos Jovens
24 a 27 de setembro de 2024 – Balneário Camboriú/SC

2.4 Boundary Conditions and Mesh Discretization

Physical and drainage boundary conditions were set to accurately simulate real embankment conditions under plane strain. For the physical boundary conditions, horizontal (U1=0) and vertical (U2=0) displacements were fixed at the bottom, while horizontal displacement (U1=0) was constrained at the right and left sides. Throughout the simulation, the soft soil surface maintained a zero-pore pressure (U8=0) as part of the drainage boundary conditions.

Figure 2 illustrates the physical boundary conditions and mesh configuration of the numerical model with a 5 m thick layer of soft soil. The mesh has been refined particularly in areas where significant stresses and strains are expected.
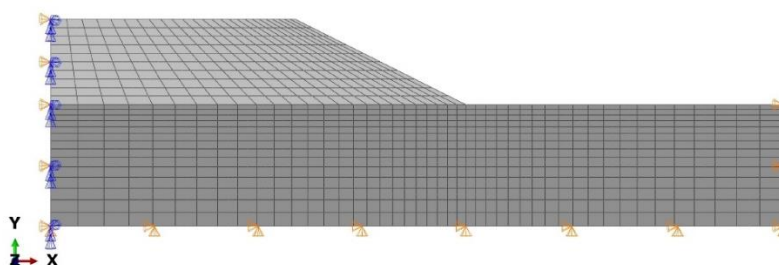

Figure 2. Boundary conditions and mesh discretization.

The numerical model used finite elements of type CPE8R (a quadrilateral flat deformation element with 8 nodes, bi-quadratic displacement, and reduced integration) for the embankment domain, and CPE8RP (a quadrilateral flat deformation element with 8 nodes, bi-quadratic displacement, bilinear pore pressure, and reduced integration) for the foundation domain.

2.6 Parametric Analysis

To investigate the effect of soil parameter variation on embankment performance, 40 analyses were performed, with 10 analyses for each numerical model. The parameters varied included the slope of the critical state line (M), the recompression index (κ), the overconsolidation ratio (OCR), and the soft soil thickness (H_s). Table 2 shows the parameters varied for each analysis and their respective values. Analysis 1 used parameters set to reference values, while subsequent analyses varied individual parameter values while holding others constant.

Table 2. Parametric analysis.

Analysis	M	Analysis	κ	Analysis	OCR
Analysis 1 (reference)	**1.0**	**Analysis 1**	**0.065**	**Analysis 1**	**1.00**
Analysis 2	1.1	Analysis 5	0.050	Analysis 8	0.75
Analysis 3	1.2	Analysis 6	0.080	Analysis 9	1.50
Analysis 4	1.3	Analysis 7	0.095	Analysis 10	3.00

The effective stress and pore pressure results were evaluated over time, depth, and width. Figure 3 shows 11 designated points (A, B, C, D, E, F, G, H, I, J, and K) along with three horizontal lines (LH1, LH2, and LH3) and six vertical lines (LV1, LV2, LV3, LV4, LV5, and LV6) where data extraction from Abaqus to Excel was performed. Point data analysis was performed over time, horizontal line data analysis was performed over width, and vertical line data analysis was performed over depth.
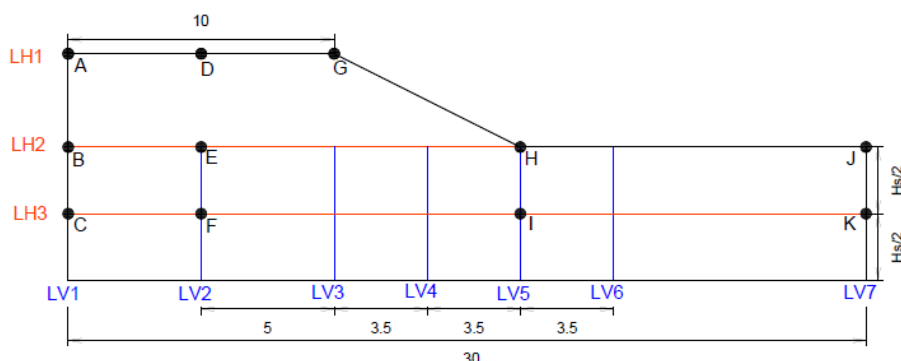
1924

XXI Congresso Brasileiro de Mecânica dos Solos e Engenharia Geotécnica
X Simpósio Brasileiro de Mecânica das Rochas
X Simpósio Brasileiro de Engenheiros Geotécnicos Jovens
24 a 27 de setembro de 2024 – Balneário Camboriú/SC

Figure 3. Points and lines of interest for data extraction, in m.

3   RESULTS AND DISCUSSION

This section examines the effect of the overconsolidation ratio, recompression index and slope of the critical state line on pore pressure and effective vertical stress along the vertical lines LV1, LV2 and LV5, and the horizontal line LH3 at 1 month and 48 months. Figure 4 shows the spatial distribution of excess pore pressure across the model domain for Analysis 1 (the reference case). The red regions indicate areas of maximum pore pressure values. At 1 month, the maximum excess pore pressure was 32.16 kPa near the base of the symmetry axis. By the 48 months mark, the excess pore pressure had completely dissipated, with values approaching zero, as shown in Figure 4b. Consequently, the results shown in the following figures correspond to a period of 1 month. On the other hand, it is important to emphasize that the bottom of the model is impermeable.

Due to space limitations, only selected typical figures are presented. However, the discussions cover the behavior observed in all 40 analyses performed.
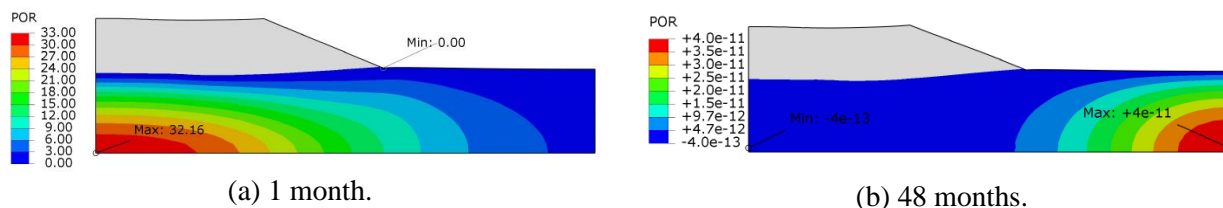
(a) 1 month.

(b) 48 months.

Figure 4. Spatial distribution of excess pore pressure.

Figure 5 shows the normalized pore pressure ($\Delta u/q$) as a function of soil depth (z/H_s), where q represents the embankment surcharge at the soft soil surface ($\gamma H_e = 70$ kPa). Figures 5a and 5b show the influence of the parameter κ on $\Delta u/q$ along the lines LV1, LV5 and LV2 for analyses with $H_s = 20$ m. In addition, Figure 5b shows the influence of H_s on $\Delta u/q$ along the lines LV1 and LV5 for analyses with $\kappa = 0.095$.

For all vertical lines, $\Delta u/q$ increases along the depth, with lines LV1 and LV5 showing a similar trend that differs from that of line LV2. Additional analysis is required to understand the differences in the behavior of the $\Delta u/q$-curves along the LV2 line compared to the curves on the LV1 and LV5 lines, given the intermediate position of LV2 between LV1 and LV5. In lines LV1 and LV5, the $\Delta u/q$ tends to increase linearly with shallower depths and stabilize at greater depths. In contrast, in line LV2, $\Delta u/q$ exhibit a non-linear increase with depth before stabilizing at greater depths. As expected, all analyses showed higher $\Delta u/q$ values along the LV1 line (symmetry axis).

At shallower depths, most analyses indicate that the $\Delta u/q$ values on line LV2 are lower than those on line LV5. Conversely, the opposite behavior is observed at greater depths. In analyses varying M, an increase in H_s from 5 m to 20 m results in the normalized depth (z/H_s) at which the $\Delta u/q$ values on lines LV2 and LV5 become equal increasing from 0.55 to 0.79. Similarly, in analyses where κ is varied, increasing H_s from 5 m to 20 m leads to the normalized depth (z/H_s) at which the $\Delta u/q$ values on lines LV2 and LV5 become

1925

XXI Congresso Brasileiro de Mecânica dos Solos e Engenharia Geotécnica
X Simpósio Brasileiro de Mecânica das Rochas
X Simpósio Brasileiro de Engenheiros Geotécnicos Jovens
24 a 27 de setembro de 2024 – Balneário Camboriú/SC

equal increasing from 0.45 to 0.84. Additionally, in analyses varying OCR, an increase in H_s from 5 m to 20 m causes the normalized depth (z/H_s) at which the $\Delta u/q$ values on lines LV2 and LV5 become equal to increase from 0.60 to 0.78.

The variation of parameter M has practically no influence on pore pressure for any soil thickness, and the effect of OCR on pore pressure is only detectable for $H_s = 5$ m, where an increase in OCR causes a decrease in pore pressure. The primary factor influencing the variation of $\Delta u/q$ along z/H_s is κ, with increasing κ corresponding to increasing values of $\Delta u/q$. Moreover, the effect of κ variation on $\Delta u/q$ tends to increase with increasing H_s. In all analyses, for a given z/H_s and vertical line, the $\Delta u/q$ values exhibit an increasing trend with increasing H_s. This pattern is attributed to the drainage path.
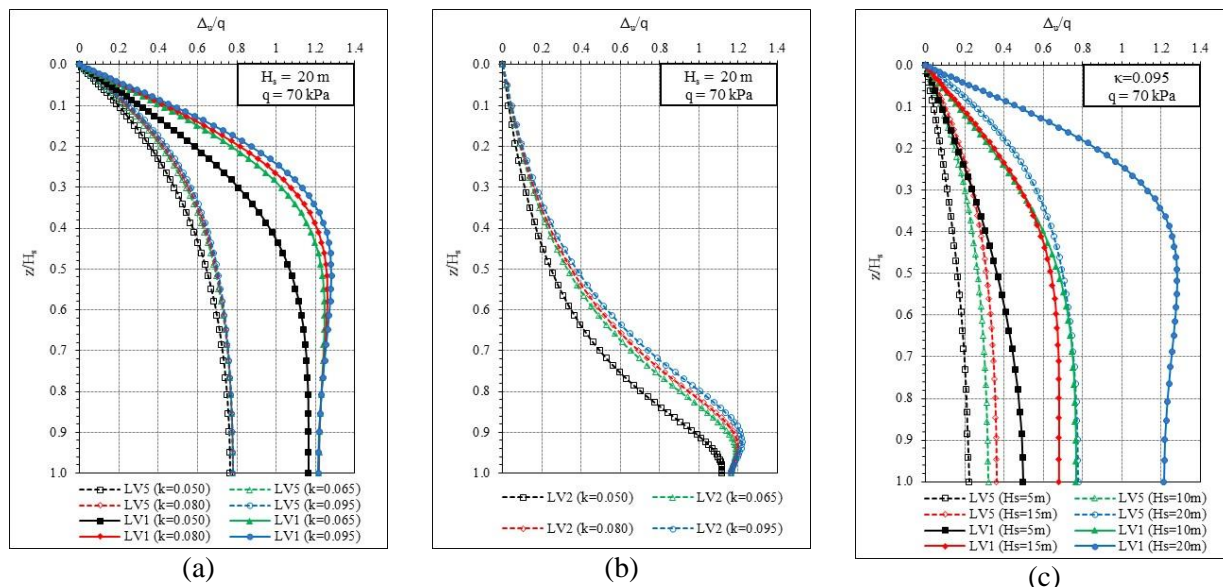

Figure 5. Variation of $\Delta u/q$ versus z/H_s.

Figure 6 illustrates four distinct normalizations used to assess the effects of varying κ, M and OCR on pore pressure along the horizontal line LH3 at the end of embankment construction (1 month). The first normalization ($\Delta u/\sigma'_v$) consists of dividing the excess pore pressure by the vertical effective stress at the end of embankment construction. The second normalization ($\Delta u/\sigma'_{v0}$) divides the excess pore pressure by the initial vertical effective stress (geostatic condition). In the third normalization ($\Delta u/\Delta\sigma'_v$), the excess pore pressure is divided by the change in vertical effective stress during the embankment construction. The fourth normalization examines the degree of consolidation (U) defined as $1 - \Delta u/q$. It is important to note that the discussion includes the results of all simulations, although the figures only show the results of analyses with H_s of 15 m.

Normalization curves of $\Delta u/\sigma'_v$ show a slower rate of decrease for $\Delta u/\sigma'_v$ in the soil region beneath the embankment compared to the soil region outside the embankment. The $\Delta u/\sigma'_v$ values decrease from their maximum near the symmetry axis to their minimum near the right side of the model. A similar pattern is observed in the curves of $\Delta u/\sigma'_{v0}$, albeit with a higher rate of decrease along the horizontal line compared to the curves of $\Delta u/\sigma'_v$.

For $H_s \geq 10$ m, both $\Delta u/\sigma'_v$ and $\Delta u/\sigma'_{v0}$ values tend to decrease with increasing H_s, especially in the soil region below the embankment. Except for analyses with $H_s = 5$ m, variations in M and OCR have minimal effect on $\Delta u/\sigma'_v$ and $\Delta u/\sigma'_{v0}$ values. However, for analyses with $H_s = 5$ m, increases in M and OCR lead to decreases in $\Delta u/\sigma'_v$ and $\Delta u/\sigma'_{v0}$ values. Conversely, an increase in κ results in an increase in $\Delta u/\sigma'_v$ and a decrease in $\Delta u/\sigma'_{v0}$ in the soil region beneath the embankment. Most analyses show $\Delta u/\sigma'_v$ values below 0.84, but higher values exceeding 1 were observed in some analyses with $H_s = 5$ m, as well as in some analyses with $H_s = 20$ m and OCR values of 0.080 and 0.095. In the soil region beneath the embankment, $\Delta u/\sigma'_{v0}$ tends to exceed 1, particularly in analyses with H_s of 5 m and 10 m. It is important to note that higher $\Delta u/\sigma'_v$

XXI Congresso Brasileiro de Mecânica dos Solos e Engenharia Geotécnica
X Simpósio Brasileiro de Mecânica das Rochas
X Simpósio Brasileiro de Engenheiros Geotécnicos Jovens
24 a 27 de setembro de 2024 – Balneário Camboriú/SC

values indicate a lower degree of soil consolidation and, depending on where they occur, instability may be present in these areas (beneath the embankment slope).
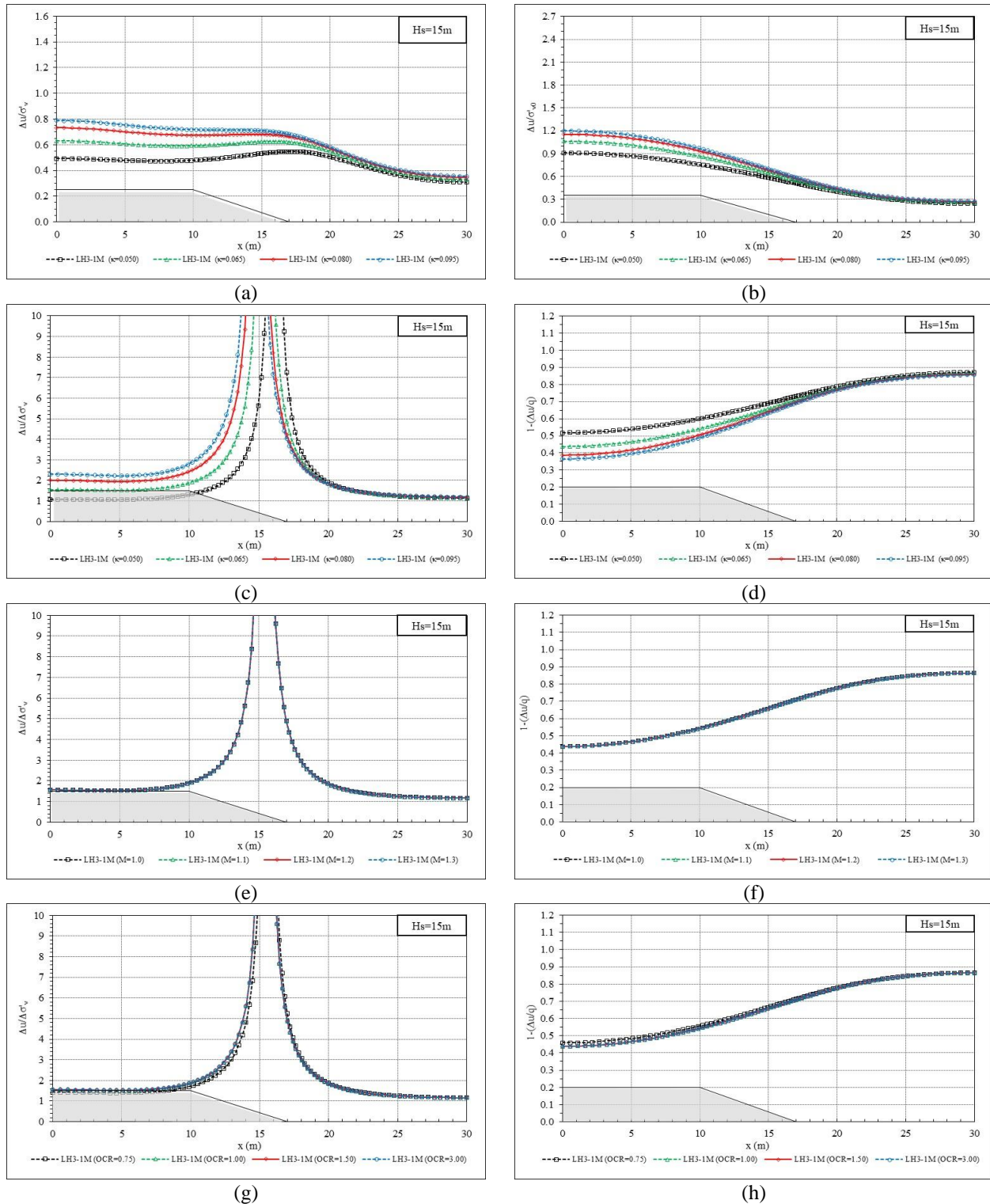

Figure 6. Variation of normalized excess pore pressure and degree of consolidation along the LH3 line.

The variation of $\Delta u/\Delta\sigma'_v$ along the horizontal line LH3 exhibits two distinct patterns. Firstly, relatively constant $\Delta u/\Delta\sigma'_v$ values below 3 were observed along the LH3 section beneath the embankment crest and outside the embankment. Secondly, peaks in $\Delta u/\Delta\sigma'_v$ values greater than 10 were observed along the LH3

XXI Congresso Brasileiro de Mecânica dos Solos e Engenharia Geotécnica
X Simpósio Brasileiro de Mecânica das Rochas
X Simpósio Brasileiro de Engenheiros Geotécnicos Jovens
24 a 27 de setembro de 2024 – Balneário Camboriú/SC

section beneath the embankment slope. It can be postulated that elevated values of $\Delta u/\Delta\sigma'_v$ may indicate the formation of a shear zone, which is linked to instability and significant deformation. Consequently, these regions demand careful monitoring and attention.

In all analyses, $\Delta u/\Delta\sigma'_v$ tend to increase with increasing H_s, especially in the soil region beneath the embankment. Variations in M and OCR have minimal effect on $\Delta u/\Delta\sigma'_v$ values. The variation of these parameters (M, OCR and κ) does not impact the $\Delta u/\Delta\sigma'_v$ values in the unloaded soil region near the model's right boundary, as expected. An increase in κ results in an increase in $\Delta u/\Delta\sigma'_v$ in the soil region beneath the embankment.

In theory, the dissipation of excess pore pressure during the consolidation process results in a corresponding increase in effective stress. Based on that, it can be concluded that in the soil region beneath the crest of the embankment, the increase in effective stress during the consolidation phase can reach up to three times the value of the increase in effective stress during embankment construction. In contrast, in the soil region beneath the embankment slope, the increase in effective stress during the consolidation can surpass ten times the value of the increase in effective stress during embankment construction.

Along the LH3 line, the degree of consolidation (U) increases as it moves away from the axis of symmetry (between 0.35 and 0.45), reaching values between 0.8 and 1.0 at the model's right boundary. It is noteworthy that consolidation degrees close to one indicate complete dissipation of excess pore pressure or the end of the consolidation process.

In all analyses, U values tend to increase with decreasing H_s, especially in the soil region near the right boundary. Variations in M, κ and OCR have minimal effect on U.

4   CONCLUSIONS

The study conducted 40 numerical simulations on 4 unreinforced embankments on soft soils to investigate the influence of parameters M, OCR, and κ, as well as the thickness of the soft soil on the variation of pore pressure, effective vertical stress, and degree of compaction. The key conclusions are presented below:

- the behavior of the $\Delta u/q$-curve along the depth changes according to the position of the analyzed vertical line. The Δu curves for lines LV1 and LV5 display similar trends, which contrast with the behavior observed in line LV2, located between them;
- the variation in M has negligible impact on pore pressure across any soil thickness, while the effect of OCR on pore pressure is only notable for $H_s = 5$ m, where higher OCR leads to reduced pore pressure. The primary factor affecting the variation of $\Delta u/q$ along z/H_s is κ, where increasing κ leads to higher $\Delta u/q$ values;
- for $H_s \geq 10$ m, $\Delta u/\sigma'_v$ and $\Delta u/\sigma'_{v0}$ values decrease with increasing H_s, especially beneath the embankment. Variations in M and OCR minimally impact these values, except in analyses with $H_s = 5$ m, where increases in M and OCR reduce $\Delta u/\sigma'_v$ and $\Delta u/\sigma'_{v0}$. Conversely, increasing κ increases $\Delta u/\sigma'_v$ and decreases $\Delta u/\sigma'_{v0}$ beneath the embankment;
- $\Delta u/\Delta\sigma'_v$ tend to increase with increasing H_s, especially in the soil region beneath the embankment. Variations in M and OCR have minimal effect on $\Delta u/\Delta\sigma'_v$ values. The variation of these parameters (M, OCR and κ) does not impact the $\Delta u/\Delta\sigma'_v$ values in the unloaded soil region near the model's right boundary, as expected. An increase in κ results in an increase in $\Delta u/\Delta\sigma'_v$ in the soil region beneath the embankment;
- U values tend to increase with decreasing H_s, especially in the soil region near the right boundary. Variations in M, κ and OCR have minimal effect on U;
- the quality of the analysis underscores the capability of Abaqus software in assessing the performance of geotechnical structures that require monitoring of excess pore pressure.

XXI Congresso Brasileiro de Mecânica dos Solos e Engenharia Geotécnica
X Simpósio Brasileiro de Mecânica das Rochas
X Simpósio Brasileiro de Engenheiros Geotécnicos Jovens
24 a 27 de setembro de 2024 – Balneário Camboriú/SC

REFERENCES

Baran, Karin. *Propriedades geotécnicas de compressibilidade de uma argila mole de Itajaí, SC*. 2014. 334 f. Dissertação (Mestrado) – Curso de Engenharia Civil, Universidade Federal de Santa Catarina, Florianópolis, 2014.

Baroni, Marcos. *Comportamento geotécnico de argilas extremamente moles da baixada de Jacarepaguá, RJ*. 2016. 321 f. Tese (Doutorado) - Curso de Engenharia Civil, Universidade Federal do Rio de Janeiro, Rio de Janeiro, 2016.

Budhu, Muni. *Soil Mechanics and Foundations*. 3rd edition. 2010.

Coutinho, R Q. *Aterro experimental instrumentado levado à ruptura sobre solos orgânicos – Argilas moles da Barragem de Juturnaíba*. Tese (Doutorado em Engenharia Civil) COPPE/UFRJ, Rio de Janeiro, 1986.

De Freitas. *Análise numérica do comportamento do aterro sobre solo mole executado na obra do Hospital da Mulher do Recife-PE*. Dissertação (Mestrado) – Universidade Federal de Pernambuco. CTG. Programa de Pós-Graduação em Engenharia Civil, 2019.

Dominoni, Claudia. *Análise de estabilidade e compressibilidade de um aterro sobre solo mole no Porto de Suape, região metropolitana do Recife*. Projeto de graduação – UFRJ. Escola Politécnica. Curso de Engenharia Civil, 2011.

Oliveira, Henrique de. *Comportamento de aterros reforçados sobre solos moles levados à ruptura*. 2006. 507 f. Tese (Doutorado) - Curso de Engenharia Civil, Universidade Federal do Rio de Janeiro, Rio de Janeiro, 2006.

Ortigão, J. A. R. *Introdução à Mecânica dos Solos dos Estados Críticos*. 3. ed. [Rio de Janeiro]: Terratek, 2007.

Terzaghi, K. (1925) Erdbaumechanick, Viena, Franz Deutcke, Áustria.

Terzaghi, K. e Frölich, O. K. (1936) *Thoerie der setzung von tonschichten*. Franz Deuticke, Leipzig.